

Seismic SSI Incoherency Effects for CANDU Reactor Building Structure

Dan M. Ghiocel

GP Technologies, Inc., 6 South Main St., 2nd Floor, Pittsford, New York 14534, USA,
Email: dan.ghiocel@ghiocel-tech.com

Georger Stoyanov

AECL Ltd., 2251 Speakman Drive, Mississauga, Ontario, Canada
Email: stoyanovg@aecl.ca

Sudip Adhikari

AECL Ltd., 2251 Speakman Drive, Mississauga, Ontario, Canada
Email: adhikaris@aecl.ca

Tarek Aziz

AECL Ltd., 2251 Speakman Drive, Mississauga, Ontario, Canada
Email: azizt@aecl.ca

ABSTRACT

The paper presents results obtained from a sequence of SSI studies for the CANDU 6 Reactor Building (RB) founded on a stiff soil deposit and a hard-rock formation. The analysis were performed using the RB stick model and an enhanced high-frequency RB model for which the containment structure (CS) is modeled more realistically by shell elements. Seismic inputs were defined by site-specific UHS that have a higher frequency content than site-independent GRS such as CSA N289.3[5], RG 1.60 or Newmark-Hall NUREG-0098. The seismic motion incoherency effects were studied using SSI methodologies validated by EPRI [1]. The 2007 Abrahamson hard-rock plane-wave coherency model was considered. The effect of wave passage is also investigated. The coherent and incoherent SSI results were compared in terms of acceleration transfer function (ATF) and in-structure response spectra (ISRS) at different locations for the internal structure (IS) and within the RB structure. The ATF and ISRS results indicated significant reductions in high-frequency range due to incoherency effects. It was noted that the type of modeling of CS influences the CS-IS coupling at the frequency associated with the torsional behaviour of the IS. If shell elements are used instead of beams an additional spectral peak is noted for the ISRS computed for CS.

SSI METHODOLOGY ACCOUNTING FOR INCOHERENCY

For performing the incoherent SSI analysis we used the ACS SASSI code [2] that includes both rigorous stochastic and approximate deterministic approaches for performing incoherent SSI analyses. The theoretical basis of the implemented incoherent SSI approaches and the free-field motion incoherency models are provided by two EPRI studies [1, 3].

Stochastic simulation approach (similar to Monte Carlo simulation used for probabilistic analyses) is based on performing statistical SSI analyses for a set of random field realizations of the incoherent free-field motion input. It respects in all details the SSI physics. It computes the mean of incoherent SSI responses, but also produces information on the scatter of these responses. It is recommended for both simple and complex SSI models with either rigid or flexible foundations.

Deterministic approaches based on approximate simple rules for combining the incoherency modes (AS approaches) or modal SSI responses (SRSS approaches). These deterministic approaches approximate the

mean of incoherent SSI responses, but offer no information on the SSI response variability. They are recommended for simple stick models with rigid basemats as applied in the EPRI incoherent SSI benchmark studies [1].

For this investigation, we used mainly the AS deterministic approach. We used the stochastic simulation approach only for checking some sample results. For the simple stick models with rigid mats both approaches provided practically identical results, as also shown in EPRI studies [1].

In addition to incoherency effects, we investigated the wave passage effects by assuming an apparent wave speed in horizontal plane in the direction of X-axis. The effects of wave passage are similar to incoherency effects by reducing translational motions and amplifying rotational motions.

CASE STUDIES

The CANDU 6 RB structure is shown in Figure 1a. Two RB structural models were used: i) the RB Stick model and ii) an enhanced high-frequency RB model for which the containment wall and dome are modeled more realistically by shell elements. The two models are shown in Figures 1b and 1c respectively. It should be noted that the CANDU 6 RB has a foundation diameter size of about 140 ft.

For site conditions we considered two soil profiles: i) a halfspace stiff soil profile with $V_s = 3,000.0$ fps and ii) a halfspace rock profile with $V_s = 5,500$ fps. For each site condition, the seismic control motion is different and the UHS are consistent with the site conditions. The seismic inputs were defined by two site-specific UHS inputs that have higher frequency content than site-independent GRS such as CSA N289.3[5], RG 1.60 or Newmark-Hall NUREG-0098. Figure 2 shows the site-specific UHS used for the two different selected site conditions. For the stiff soil profile PGA is 0.41g and for the rock profile it is 0.32g. The UHS plots correspond to an annual occurrence probability of 1.0×10^{-4} . It should be noted that for the soil site the UHS curve has a spectral peak at 10 Hz, while for the rock site the UHS curve has a top spectral plateau between 20 Hz and 40 Hz.

The two 2007 Abrahamson plane-wave coherency models developed for hard-rock sites and soil sites were considered [4]. The two rock and soil coherency models are described in Figure 3. The effect of wave passage was also investigated by assuming site-specific apparent horizontal velocities of seismic waves, namely, 7,000 fps for the soil site and 10,000 fps for the rock site.

RESULTS

Figures 4 and 5 show the effects of motion incoherency on the 5% damping ISRS computed at the top of Internal Structure (IS) for the X and Z directions. For the soil site the horizontal ISRS has a much larger spectral peak than for the rock site since the two UHS inputs have a very different spectral content. The UHS for the soil site has much larger amplitude at the 6.5 Hz spectral peak.

Figure 4 shows the ISRS results for the rock site and Figure 5 shows the ISRS results for the soil site. The effect of incoherency is significant in both cases. For the horizontal ISRS, the effect of incoherency manifests for the rock site by reducing the spectral peak at 25 Hz, and for soil site by reducing the spectral peak at 6.5 Hz. For vertical ISRS, this is visible for frequencies higher than 10 Hz for the rock site and higher than 2-3 Hz for the soil site.

Figures 5 and 6 also compares the ISRS computed using the RB Stick model (Figure 1b) vs. the RB Shell model (Figure 1c). For horizontal ISRS, the results obtained with the two models match very well for coherent inputs. For the incoherent input, the Shell model indicates a slightly larger incoherency effect for

the soil site. For vertical ISRS the results obtained using the Stick and Shell models we noted some differences, especially for the soil site.

Figures 6 and 7 show the ISRS computed for the Shell model at the top of Containment Shell (CS) for all 24 node locations around the ring beam in the horizontal direction. It should be noted that the effect of incoherency appears to reduce the scatter among the 24 nodes. In order to compare with the Stick model results in Figures 4 and 5 we used the average of the 24 ISRS curves.

Figures 8 and 9 show the effects of wave passage in the X-direction. The acceleration transfer function (ATF) amplitude plots indicate that the wave passage effects are negligible. For the soil site, the wave passage effects are visible only in the high-frequency range above 15 Hz, as shown in Figure 9 (right plots).

Finally, Figures 10 and 11 show the ISRS results at the Basemat Center for all case studies, including coherent, incoherent, incoherent with wave passage for the Stick and Shell models. It should be noted that at the basemat level the effects of incoherency are significantly larger for the rock site since they manifest more pronounced in the high-frequency range than in the middle frequency range.

CONCLUSIONS

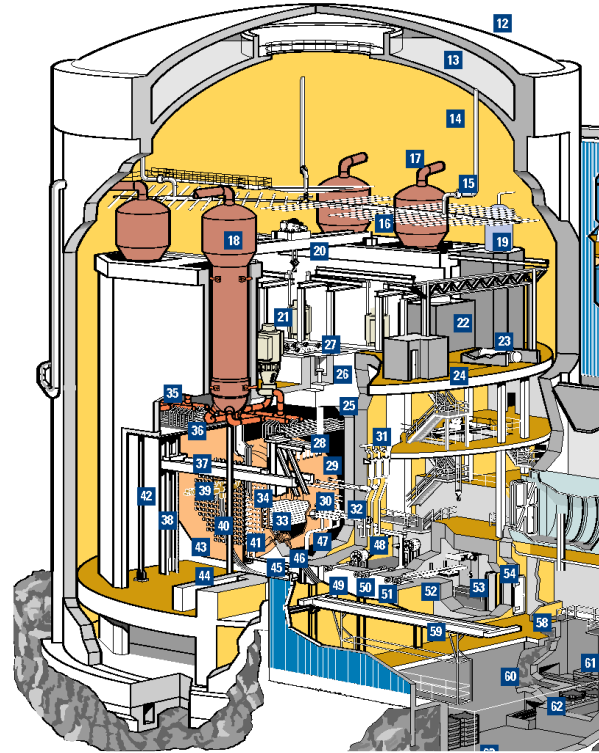
The paper shows that the incoherency effects are significant for the case studies included in the paper, namely, a stiff soil site case and a rock site case. The effects of wave passage appear to be insignificant for the two cases studies.

The effect of structural modeling the CS by shell elements rather than by a simple stick changes quite visibly the ISRS at the top of IS. This is due to an increase in the dynamic coupling between the CS and IS structures. This dynamic coupling is affected by the structural modeling of the CS, although the IS model is the same. The CS-IS dynamic coupling effects appear to be larger for the Shell model, and for incoherent motions.

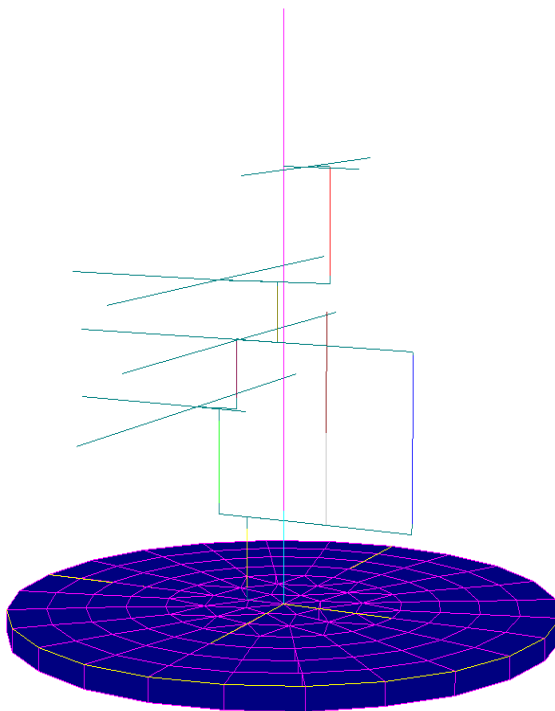
Not included in this paper is the effect of the CS structural modeling on the CS response. The results indicate a significant ISRS spectral peak due to the dynamic coupling with the IS.

REFERENCES

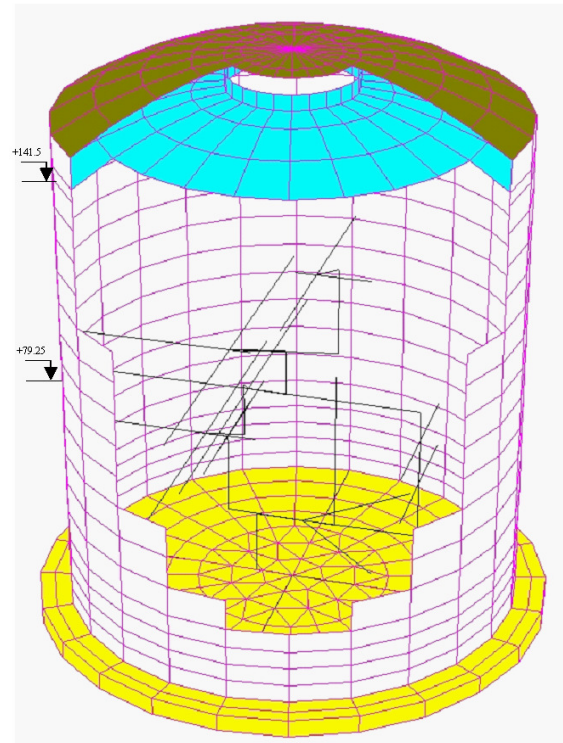
1. Short, S.A., G.S. Hardy, K.L. Merz, and J.J. Johnson. "Validation of CLASSI and SASSI to Treat Seismic Wave Incoherence in SSI Analysis of Nuclear Power Plant Structures, Electric Power Research Institute, Palo Alto, CA and US Department of Energy, Germantown, MD, Report No. TR-1015111, November, 2007
2. ACS SASSI Version 2.3.0: "An Advanced Computational Software for 3D Dynamic Analysis Including Soil Structure Interaction", Ghiocel Predictive Technologies, Inc., June, 2009.
3. Tseng and Lilhanand. "Soil-Structure Interaction Analysis Incorporating Spatial Incoherence of Ground Motions", Electric Power Research Institute, Palo Alto, CA, EPRI TR-102631, March, 1997
4. Abrahamson, N. (2007) "Effects of Seismic Motion Incoherency Effects" Electric Power Research Institute, Palo Alto, CA, EPRI TR-1015111, December 2007
5. CSA N289.3-10 Design Procedures of Seismic Qualification of Nuclear Power Plants, May 2010,



a) CANDU 6 RB Structure



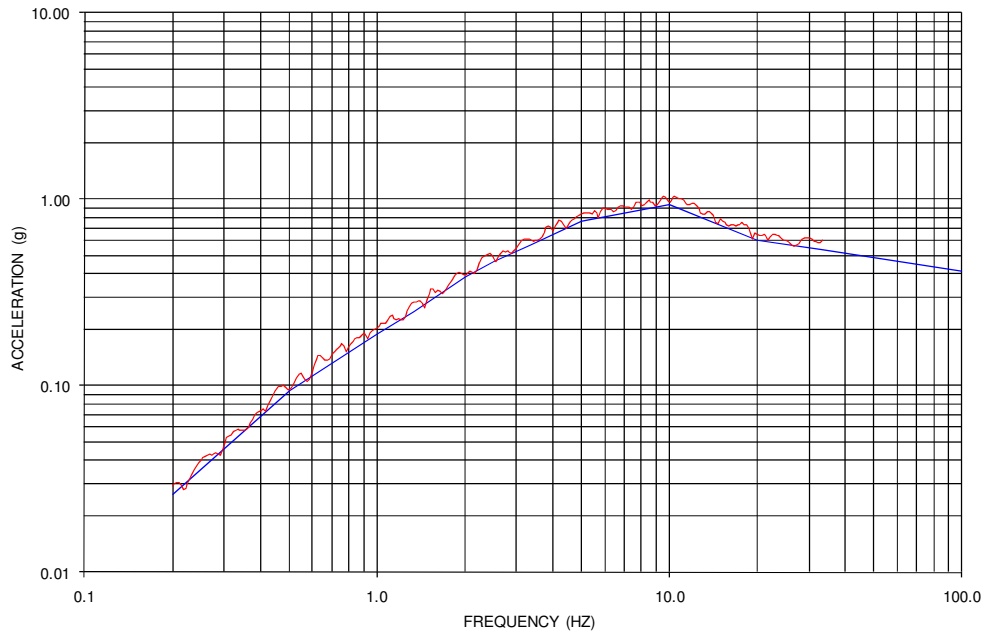
b) RB Stick Model



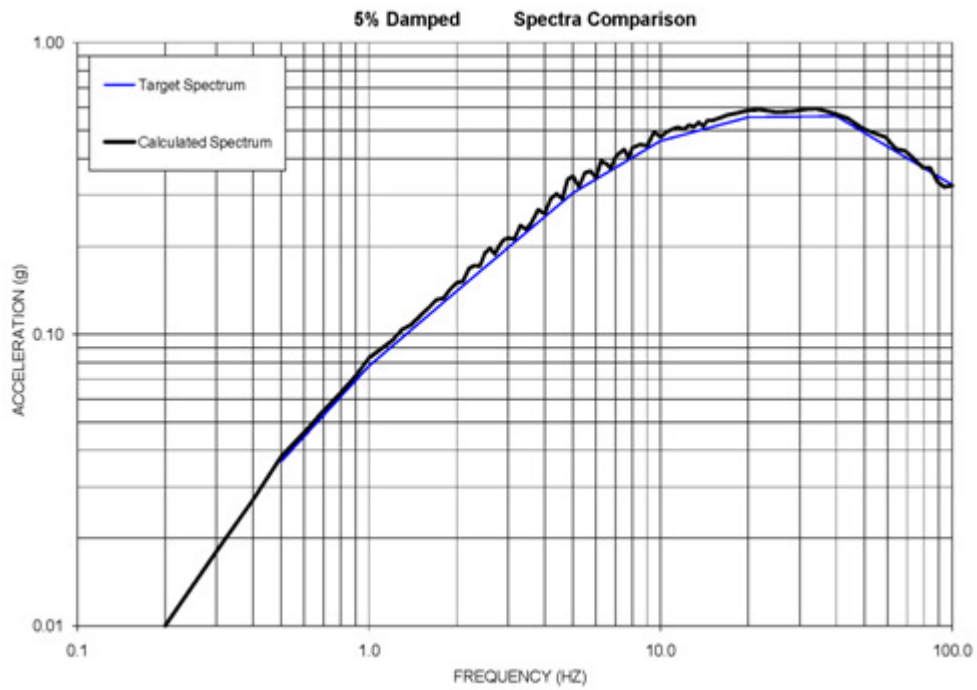
c) RB Shell Model

Figure 1 CANDU 6 RB Structure Models

5% Damped Spectra Comparison



a) UHS Input for the Soil Profile, $V_s = 3,000$ fps



b) UHS Input for the Rock Profile, $V_s = 5,500$ fps

Figure 2 Target and Computed UHS for the Two Selected Sites with Soil and Rock Profiles

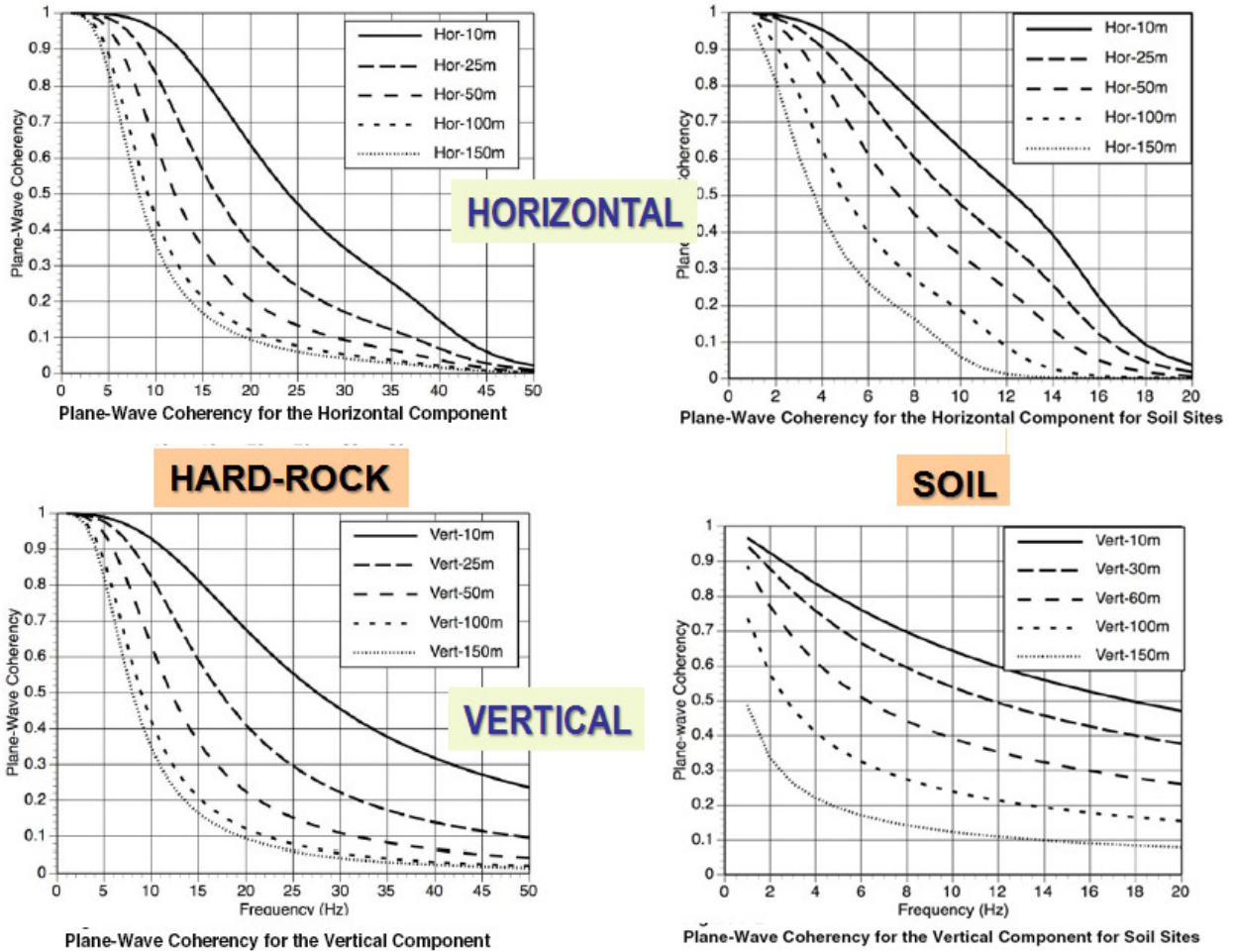


Figure 3 2007 Abrahamson Plane-Wave Coherency Models for Rock and Soil Site Conditions

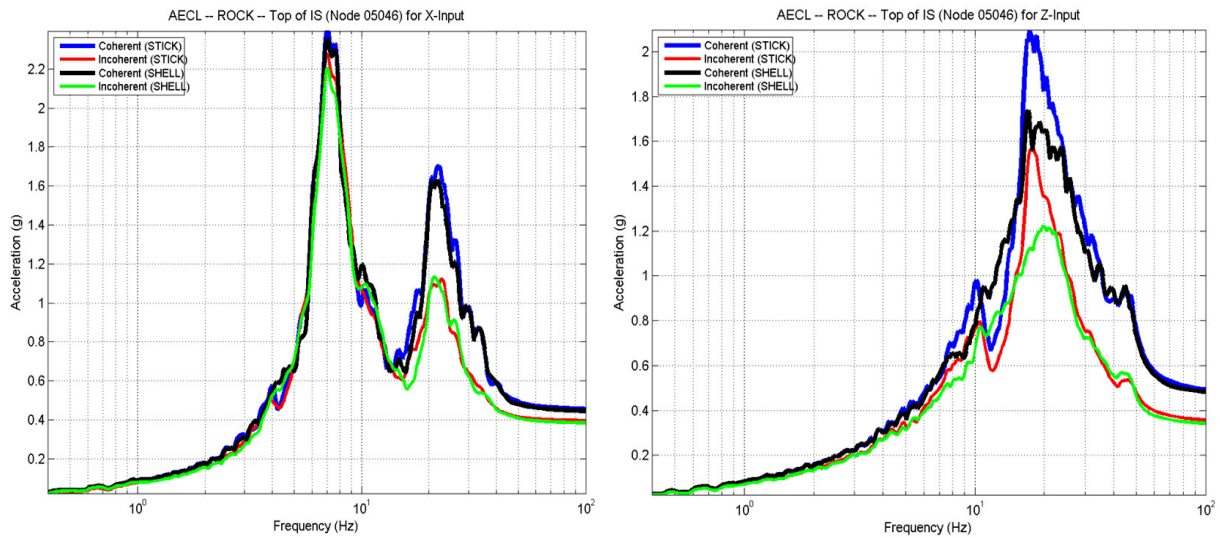


Figure 4 ISRS at Top of IS for Rock Profile in X and Z Directions; Stick Model vs. Shell Model

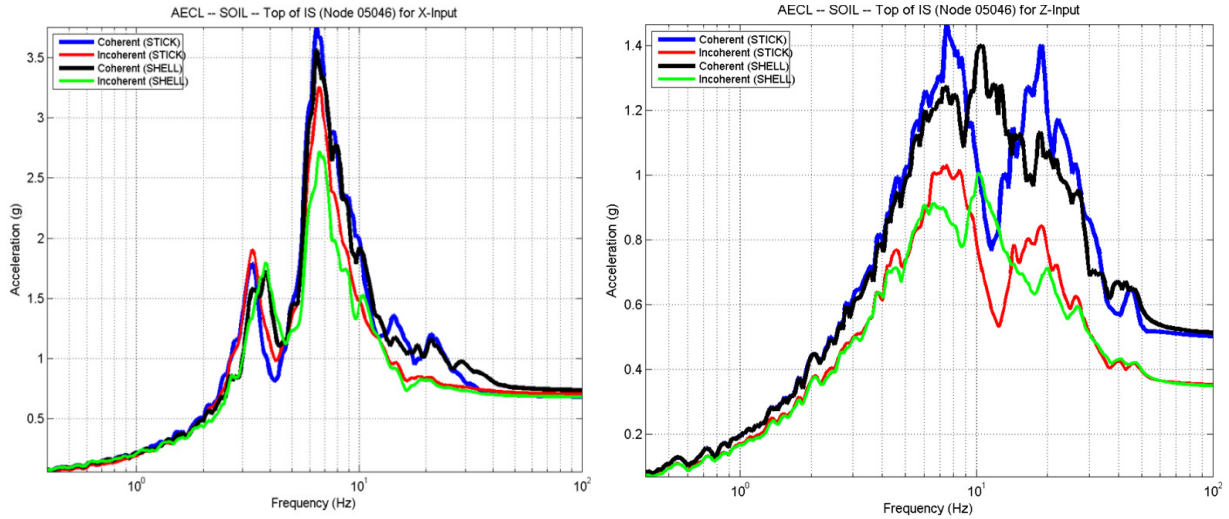


Figure 5 ISRS at Top of IS for Soil Profile in X and Z Directions; Stick Model vs. Shell Model

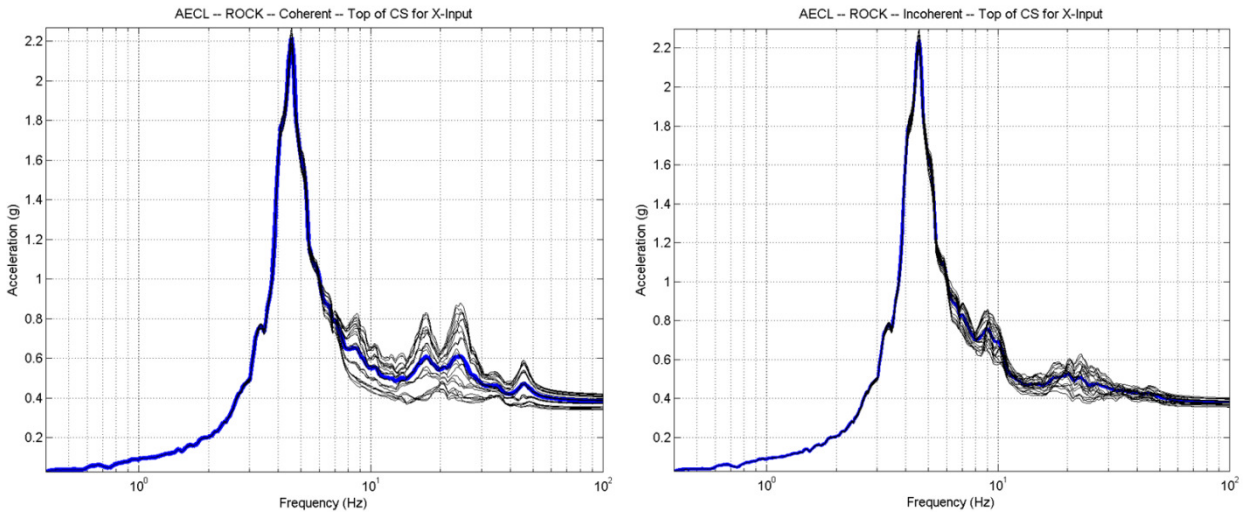


Figure 6 ISRS at Top of CS for Rock Profile in X Direction for All Ring Beam Locations - Shell Model

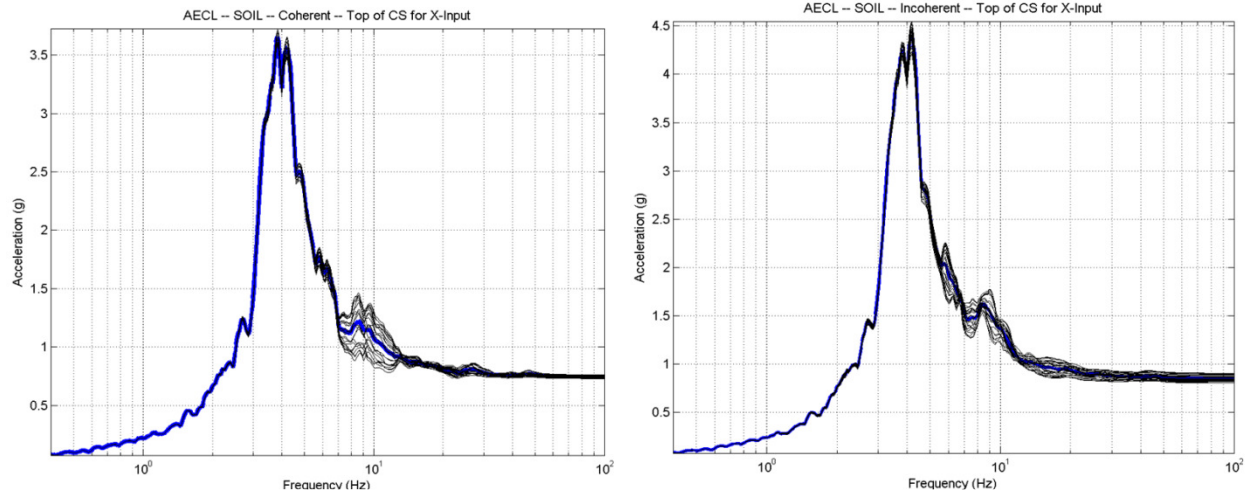


Figure 7 ISRS at Top of CS for Soil Profile in X Direction for All Ring Beam Locations - Shell Model

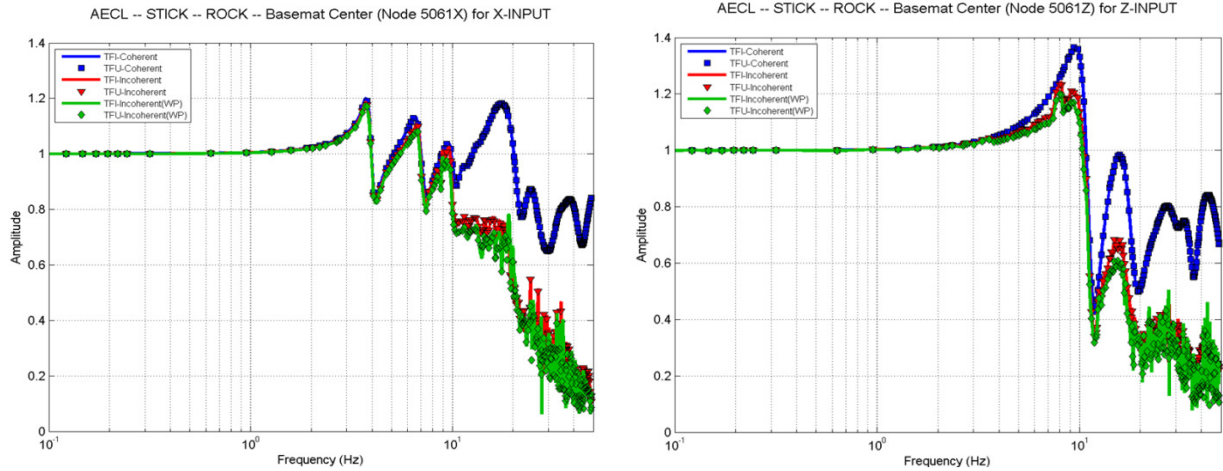


Figure 8 ATF at Basemat Center for Rock Profile in X and Z Directions Including Wave Passage Effects

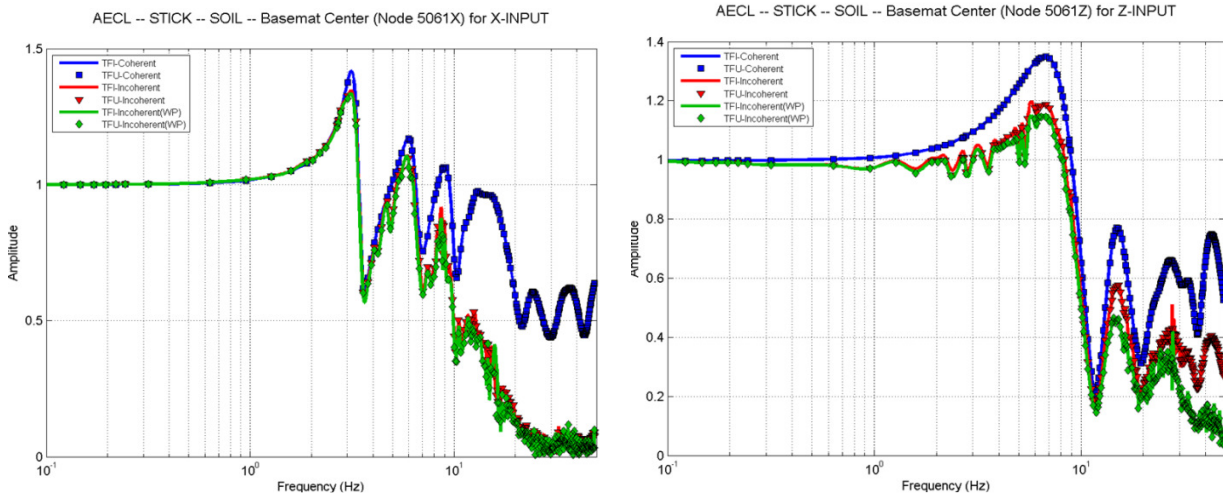


Figure 9 ATF at Basemat Center for Soil Profile in X and Z Directions; Including Wave Passage Effects

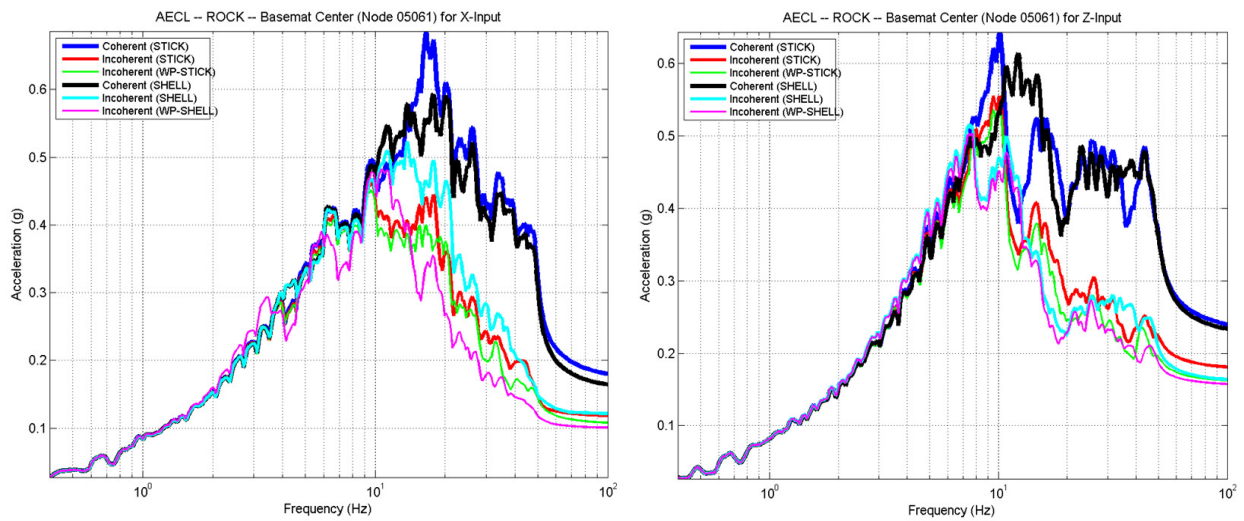


Figure 10 ISRS at Basemat Center for Rock Profile in X and Z Directions; Comparison for All Cases

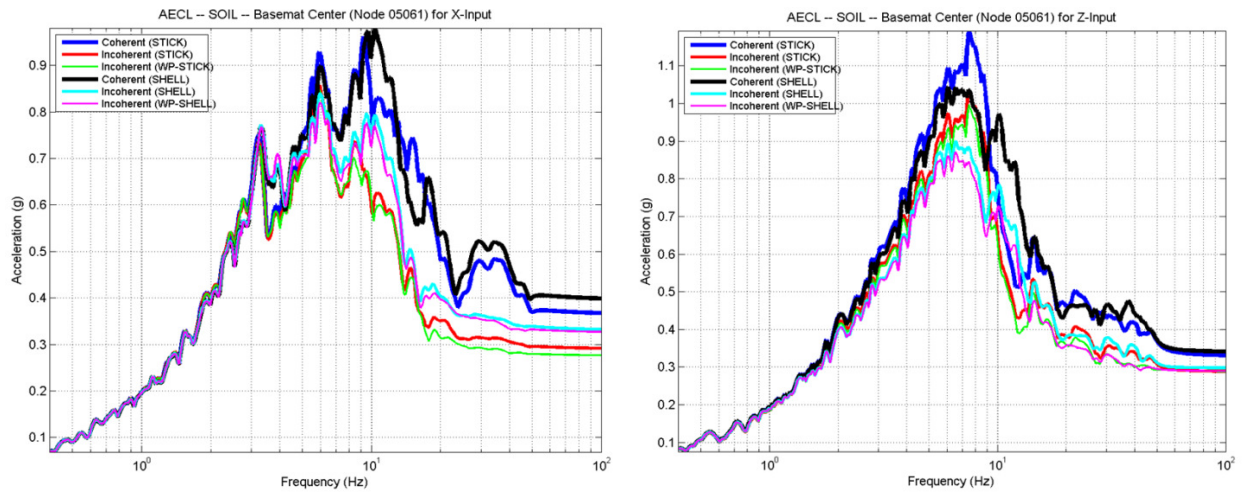


Figure 11 ISRS at Basemat Center for Soil Profile in X and Z Directions; Comparison for All Cases